Adsorption (2007) 13: 491–500
DOI 10.1007/s10450-007-9067-8

Kinetic Monte Carlo study of binary diffusion in silicalite

N. Laloué · C. Laroche · H. Jobic · A. Méthivier

Received: 3 May 2007 / Revised: 25 September 2007 / Accepted: 26 September 2007 / Published online: 23 October 2007

Abstract We report a Kinetic Monte Carlo (KMC) study of the diffusion of linear n-hexane (nC6) and 2,2-dimethylbutane (22DMB) mixture in zeolite silicalite. We first investigated the loading dependences of single component self- and corrected diffusivities of nC6 at 300 K. Anisotropic transition rates are implemented to account for the distribution of the molecules within the zeolite framework. Repulsive guest-guest interactions are modeled using the parameter introduced by Reed and Ehrlich (Surf. Sci. 102:588–601, 1981). The results are in good agreement with recent experimental Quasi Elastic Neutron Scattering data of Jobic et al. (J. Phys. Chem. B 110:2195–2201, 2006), although the influence of the adsorption isotherm inflection is not reproduced. The binary diffusion study of nC6/22DMB mixtures was performed by implementing the nC6 transition rates used for the single component study while 22DMB molecules propagate via intersection-intersection hops. This KMC model allows for different saturation capacities and accounts for interactions between molecules by introducing f_{ij} parameters. Results show the large impact of guest-guest interactions between nC6 and 22DMB on both self- and corrected diffusivities of the two components. Molecule-size effects are found to be predominant near 22DMB saturation capacity. Acceleration/deceleration effects already described in the literature are confirmed.

N. Laloué · C. Laroche (✉) · A. Méthivier
IFP-Lyon, BP 3, 69360 Solaize, France
e-mail: catherine.laroche@ifp.fr

H. Jobic
IRCELYON, Institut de Recherches sur la Catalyse et l'Environnement de LYON, CNRS, Université de Lyon, UMR5256, 2 Avenue A. Einstein, 69626 Villeurbanne, France

Keywords Molecular modeling · Separation · Zeolite · Kinetics · Diffusion coefficient

Abbreviations

a	Reed–Ehrlich parameter, dimensionless
b	Reed–Ehrlich parameter, dimensionless
b_A	Langmuir constant of the DSL model, Pa^{-1}
b_B	Langmuir constant of the DSL model, Pa^{-1}
D_{self}	self-diffusion coefficient, $m^2\ s^{-1}$
D_C	corrected diffusivity, $m^2\ s^{-1}$
f	Reed–Ehrlich parameter, dimensionless
$k_{i\rightarrow j}$	transition rates from site i to site j, s^{-1}
k_{STR}	transition rates along straight channels, s^{-1}
k_{ZZ}	transition rates along zigzag channels, s^{-1}
K	transition rates ratio, dimensionless
n	number of nearest neighbours, dimensionless
N	number of molecules, dimensionless
Q	parameter defined by (7), dimensionless
R	gas constant, $J\ mol^{-1}\ K^{-1}$
$\boldsymbol{R}(t)$	vector position of the center of mass at a time t, m
$\boldsymbol{r}_i(t)$	vector position of molecule i at a time t, m
t	time, s
T	absolute temperature, K

Greek letters

ξ	random number, dimensionless
δE	variation of the activation energy, $J\ mol^{-1}$
θ	loading or fractional occupancy, dimensionless
Θ_i	number of molecules of species i, molecules per unit cell
$\Theta_{i,sat}$	saturation capacity of specie i, molecules per unit cell
Δt	mean residence time of a given configuration, s

Subscripts

sat	referring to saturation
int	referring to intersection
str	referring to straight channel
zz	referring to zigzag channel

1 Introduction

Separation of paraffins isomers is of great industrial interest, because of its highly potential applications in the oil refinery industry. Separation induced by kinetic effects has been investigated, using zeolites as a shape selective adsorbent (Cavalcante and Ruthven 1995). The control of diffusion process, requiring a precise knowledge of self-, transport and corrected diffusivities (D_{self}, D_t and D_C, respectively) of molecules inside the nanoporous material, is essential for the design of industrial applications. Many atomically detailed studies have investigated the loading dependence of those diffusivities of small molecules (Skoulidas and Sholl 2002) or light *n*-alkanes (June et al. 1992) in the MFI-type zeolite as single component system. Binary mixtures diffusion has also been studied using those techniques but restricted to systems consisting of small molecules (Snurr and Käeger 1997; Gergidis et al. 2000). In the case of strongly-binding or tight-fitting guest-zeolite systems, residence times in adsorption sites are much longer than travel times between sites so that diffusion becomes a slow activated process. Molecular Dynamics (MD) simulation techniques do not allow the molecule to explore a representative volume of the pore space due to excessive computational time. Specific rare events techniques are required to handle separately fast and slow events by using an intrinsically discontinuous mechanism. They are related to the Markovian master equation that describes the evolution of the system as a function of time. In the case of a slow activated process, the zeolite framework can be mapped as a network or a lattice of adsorption sites and diffusion can be viewed as successive random jumps from an adsorption site to another by crossing free energy barriers. As reported by Keil et al. (2000), combining Kinetic Monte Carlo (KMC) algorithm and lattice model is the more adapted technique to study diffusion at finite loadings of poorly connected systems. By its flexibility, it allows to consider different types of sites and to account for their local environment. The jump frequencies of molecules are estimated by Transition State Theories (TST) (June et al. 1991; Dubbeldam et al. 2005) or by MD (Smit et al. 1997) and are used as input data in KMC algorithms. KMC simulations has been used to study single component loading dependence of diffusivities of benzene in NaY (Saravanan and Auerbach 1997), methane and perfluoromethane in MFI (Paschek and Krishna 2001a) and 2-methylhexane in MFI (Paschek and Krishna 2000). It has been extended to study binary mixtures diffusion of real systems such as CH_4/CF_4 in MFI (Paschek and Krishna 2001a), or hypothetical ones by imposing arbitrary transition rates (Maceiras and Sholl 2002; Paschek and Krishna 2001b). KMC has also been used to model surface growth (Metiu et al. 1992) and adsorption kinetics on surfaces (Fichthorn and Weinberg 1992).

In this paper, we report a study of the loading dependence of single-component diffusion of linear hexane (nC6) in MFI-type zeolite at 300 K, using a lattice model approach combined with KMC. We also report a study of binary diffusion at 300 K of nC6 and 2,2-dimethylbutane (22DMB) mixture in silicalite based on information coming from the single component investigation.

2 Kinetic Monte Carlo simulation methodology

In this study, the silicalite framework is represented as a three-dimensional network of intersecting straight (str) and zigzag (zz) channels. Molecules are randomly positioned on the lattice and can move from one site to the neighbouring site via hops, with a probability determined by transition rates. Moreover, local molecular interactions are taken into account by modifying the magnitude of the free energy barrier according to the methodology developed by Reed and Ehrlich (1981) and described by Krishna et al. (2004a) for KMC applications: the transition rates of a given molecule are altered depending on the number of molecules located in their nearest neighbours sites according to (1):

$$k_{i\to j}(n) = k_{i\to j}(0)\, f^n \tag{1}$$

where $f = \exp(\delta E/RT)$ is the so called Reed and Ehrlich parameter, $k_{i\to j}$ is the transition rates from site i to site j, dependent on the number of nearest neighbour occupied sites n. f can be either constant or loading dependent according to the expression $f = a\exp(b\theta)$ from Reed and Ehrlich (1981) where a and b are adjusted and θ is the fractional occupancy $\in [0-1]$. A standard KMC algorithm with variable time step is implemented to propagate the system (Fichthorn and Weinberg 1991; Saravanan and Auerbach 1997; Paschek and Krishna 2000). A hop is made every KMC step and the system clock is updated with variable time steps Δt chosen in a Poisson distribution according to

$$\Delta t = -\ln(\xi)/k_{total} \tag{2}$$

where ξ is a random number $\in [0-1]$ and k_{total} represent the sum of transition rates $k_{i\to j}$ of all possible moves at the given configuration. After each performed step, the process list is updated and the positions of the molecules

are stored for further dynamical properties calculations. Periodic boundary conditions are applied to avoid finite size effects. D_{self} is determined using (3) based on the Mean Square Displacement (MSD) of the N individual particles:

$$D_{self} = \lim_{t\to\infty} \frac{d}{dt}\frac{1}{6}\frac{1}{N}\sum_{i=1}^{i=N}\langle[r_i(t) - r_i(0)]^2\rangle \tag{3}$$

where $\boldsymbol{r}_i(t)$ represent the vector position of the particle i at a time t. D_C, also called Maxwell-Stefan diffusivity, is related to the displacement of the centre of mass of the N adsorbed particles by (4):

$$D_C = \lim_{t\to\infty} \frac{d}{dt}\left\{\frac{N}{6}\langle[R(t) - R(0)]^2\rangle\right\} \tag{4}$$

where $\boldsymbol{R}(t)$ represent the vector position of the centre of mass of the N particles at a time t. MSD calculations are performed using the order-n algorithm (Frenkel and Smit 2002; Auerbach et al. 1995), mapping the variable time scale on a periodic time scale as done in MD simulations. In order to improve CPU time, D_{self} is determined during the simulations whereas D_C is estimated afterwards by a post-treatment procedure using the stored positions of the centre of mass. Depending on occupancy, the simulations performed in this work are undergone on lattices of $6 \times 6 \times 6$ to $12 \times 12 \times 12$ unit cells and involve 10^7 to 10^9 simulation steps. Those conditions allow both to encapsulate the dynamics of the system and to provide accurate estimations of the calculated ensemble averages. Moreover, average positions of the molecules are recorded giving an indication of the average residence time distribution of molecules on each type of site. The source code developed here has been validated by quantitatively reproducing the results from literature of the loading dependence of D_{self} and D_C of CH_4 in MFI on cubic and MFI lattices (Krishna et al. 2004a) and CF_4 in MFI (Krishna et al. 2004b).

3 Loading dependence of linear n-hexane in silicalite

For understanding diffusion in zeolite, the thermodynamics of adsorption is of great importance. Molecules configuration and localization within the zeolite framework as well as the way they interact between each other provide important information for computing diffusion. Studies of adsorption of nC6, both theoretical (Vlugt et al. 1999; Pascual et al. 2003) and experimental (Song and Rees 1997), indicate that nC6 molecules can be located on three distinct types of site, intersection (int), straight (str) and zigzag (zz) channels, with a saturation capacity, $\Theta_{nC6,sat}$, of 8 molecules/u.c. According to these theoretical investigations, the adsorption isotherm is correctly modeled by a Dual Site Langmuir (DSL) model, exhibiting the presence of two distinct types of site. Nevertheless, they do not explicitly define which site among intersection, straight and zigzag sites correspond to the two types of sites revealed by the DSL model. Moreover, despite the discrepancies in the literature about the positions of the nC6 molecules below $\Theta_{nC6} = 4$ molecules per unit cell (u.c.), theoretical studies generally agree with a preferential location of nC6 molecules in both channels at high occupancy (Vlugt et al. 1999; Pascual et al. 2003).

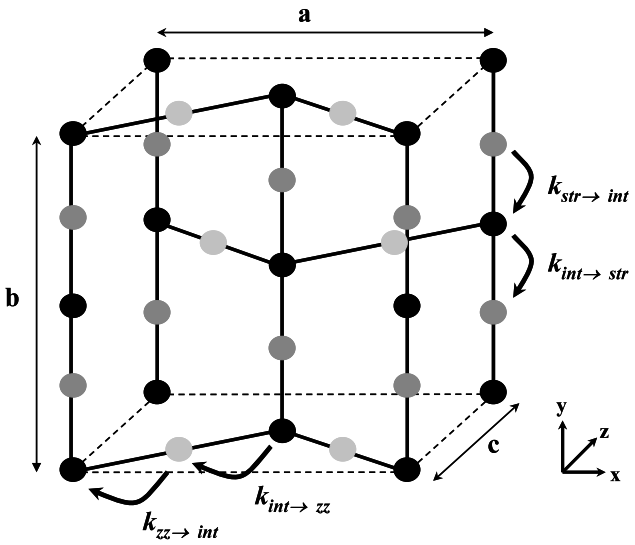

Fig. 1 Schematic of the unit cell defined for KMC simulations of nC6 in MFI. Intersections (*black dots*) are connected to straight (*dark grey dots*) and zigzag (*light grey dots*) channels. The cell parameters are $a = 2.01$ nm, $b = 1.99$ nm and $c = 1.34$ nm

In order to account for the molecule distribution at high loading, we present two different approaches based on the implementation of anisotropic transition rates. In both approaches, a discretization of the zeolite framework of 12 adsorption sites per unit cell is chosen (see schematic in Fig. 1). Local molecular interactions are taken into account by implementing several f profiles allowing either no interaction or repulsive guest-guest interactions, supported by Shuring et al. (2000) results of MD simulations that indicate a rise of repulsive molecular interactions while increasing nC6 loading. For both approaches, transition rates are adjusted at infinite dilution to reproduce the experimental zero loading D_{self} of Jobic et al. (2006), measured by Quasi Elastic Neutron Scattering (QENS). Those transition rates are summarized in Table 1. The loading dependences of the normalized diffusivities obtained from this KMC work are shown in Fig. 2 and are compared to the experimental results of Jobic et al. (2006) measured by QENS.

The first approach developed considers that the two types of sites defined by the DSL model are the intersection and the undifferentiated channel sites. This is supported by June et al. (1992) MD simulations showing that intersections sites

Table 1 Transition rates in 10^8 m^2 s^{-1} implemented in the KMC simulations of the loading dependence of D_{self} and D_C of nC6 as a single component in silicalite

	$k_{str\to int}$	$k_{int\to str}$	$k_{zz\to int}$	$k_{int\to zz}$
Approach 1	186.5	3108.0	31.1	518.0
Approach 2	129.6	6000.0	21.6	360.0

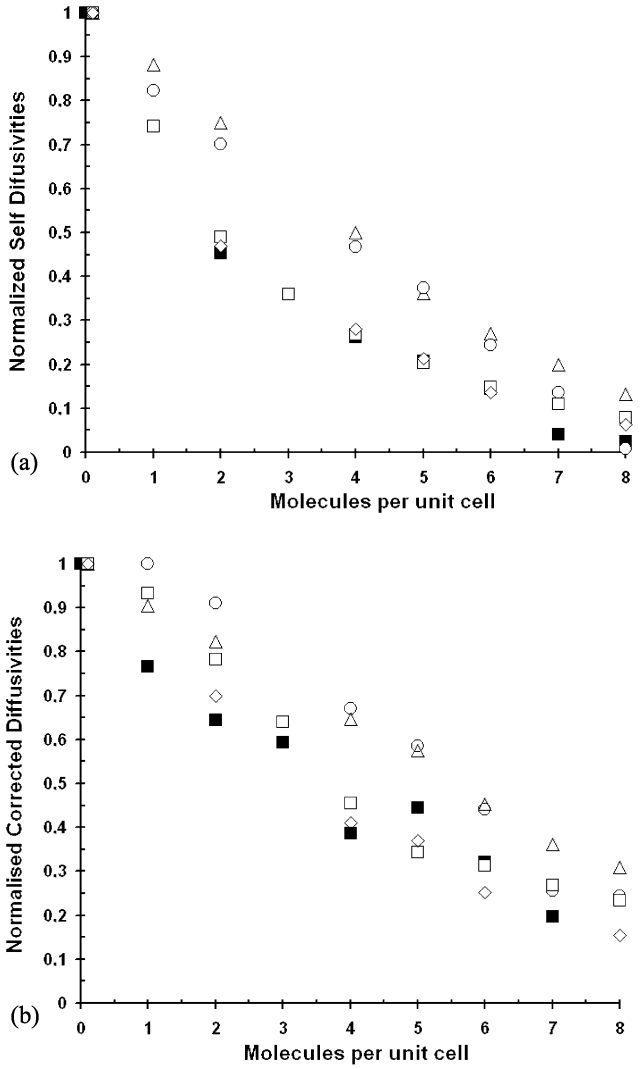

Fig. 2 Normalized self- (**a**) and corrected (**b**) diffusivities of nC6 in MFI zeolite as a function of number of molecules per unit cell. Filled squares and circles represent QENS data from Jobic et al. (2006). *Open symbols* represent KMC simulations from this work: *triangles* and *circles* correspond to approach 1 without interaction and with $f = 1.0\exp(1.05\theta)$, respectively. Results from approach 2 using $K = 16.6$ is represented by *squares* and *diamonds* implementing $f = 1.0$ and $f = 1.5$

are less energetically favourable sites than channel sites. To account for the preferential location of the nC6 molecules in channel sites at high coverage (Vlugt et al. 1999; Pascual et al. 2003), the transition probability to jump from either

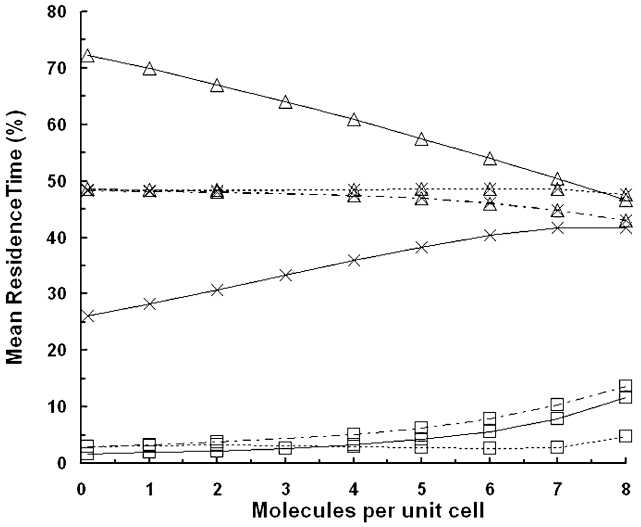

Fig. 3 Mean residence time spent by the nC6 particles in each type of sites of the MFI zeolite. *Squares* indicate intersection sites, *triangles* and *crosses* represent straight and zigzag channel sites, respectively. - – - lines correspond to approach 1 without interaction, - - - to approach 1 with molecular interactions modeled by $f = 1.0\exp(1.05\theta)$ and — to approach 2 with $K = 16.6$

channel site to an intersection site is reduced compared to the reverse jump rate, according to (5)

$$k_{str\to\mathrm{int}} = k_{\mathrm{int}\to str} b_B/b_A \quad \text{and} \quad k_{zz\to\mathrm{int}} = k_{\mathrm{int}\to zz} b_B/b_A \tag{5}$$

where b_A and b_B are the Langmuir constants of the DSL model, characterizing the adsorption at the channels sites and intersection sites, respectively. $b_A/b_B = 16.6$ at 300 K according to Jobic et al. (2006). A similar approach was used by Krishna et al. (2004b) to investigate the loading dependence of CF_4 in MFI. Besides, a ratio of 6 between transition rates in straight and zigzag directions is applied according to (6), supported by MD results (Leroy et al. 2004; Runnebaum and Maginn 1997)

$$\frac{k_{str\to\mathrm{int}}}{k_{zz\to\mathrm{int}}} = \frac{k_{\mathrm{int}\to str}}{k_{\mathrm{int}\to zz}} = \frac{k_{STR}}{k_{ZZ}} = 6 \tag{6}$$

where k_{STR} and k_{ZZ} correspond to the inverse of the mean residence time along straight and zigzag channels respectively. The results of KMC simulations shown in Fig. 2 indicate a general linear decrease of D_{self} and D_C with increasing loading up to saturation. They present a deviation from experimental data, especially for the D_{self} values. Indeed, Fig. 3 shows that molecules spend the same time in both channels whatever the loading. This is in contradiction with two generally agreed observations: nC6 molecules are trapped into zigzag channels (Zhu et al. 2001) due to their incommensurate "freezing" (Smit and Maesen 1995).

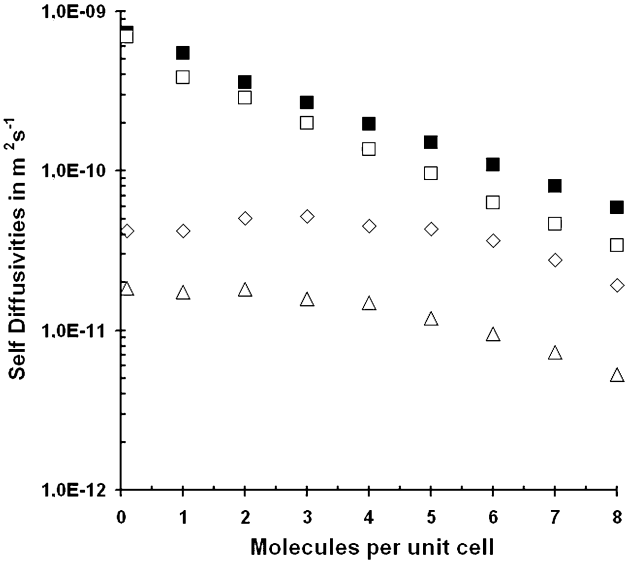

Fig. 4 Self-diffusion coefficient of nC6 in MFI determined in all crystallographic directions, represented as a function of the number of molecules. KMC simulations from the second approach using $K = 16.6$. *Filled squares* represent total self-diffusion, *open diamonds*, *squares* and *triangles* represent the self-diffusion in the x, y and z crystallographic directions, respectively. x and y directions correspond to diffusion along zigzag and straight channels, respectively

Moreover, it is well known that the diffusion along straight channels is larger than in zigzag ones (Song and Rees 1997; Koriabkina et al. 2005). Therefore, considering undifferentiated channel site is not suitable for reproducing either loading dependences of D_{self} and D_C diffusivities and molecule distribution. In addition, it is noticeable that the impact of repulsive guest-guest interactions on both D_C and D_{self} diffusivities is larger at high loadings than at low coverage. Indeed, at low loadings, the repulsive interactions of nearest neighbours are negligible as molecules spend more time in both straight and zigzag channels (cf. Fig. 3), separated from each other by an intersection site. However, as loading rises, the percentage of molecules located at the intersection increases and guest-guest interactions become effective at high loading. By increasing local transition rates, these interactions decrease the residence time of the molecules in intersection sites and thus decrease diffusivity.

In a second approach we assume that the two types of adsorption sites defined by the DSL model are the straight and the zigzag channel sites. Therefore, they are differentiated according to $k_{\text{int}\to str}/k_{\text{int}\to zz} = b_A/b_B = 16.6$. In addition, the intersection site can be considered as a "passing" site since being the least energetically favourable site. The general motion along a given channel is thus controlled by hops from channel sites towards intersection sites. Previous equation (6) can then be reduced to $k_{str\to\text{int}}/k_{zz\to\text{int}} = k_{STR}/k_{ZZ} = 6$. Moreover, in order to model the incommensurate "freezing" of the molecules in zigzag channels, the probability of leaving this site is reduced compared to the probability of its reverse jump according to $k_{\text{int}\to zz}/k_{zz\to\text{int}} = K$. Several values of K were investigated and the best results are obtained by using $K = 16.6$. The results shown in Fig. 2 are in good qualitative agreement with experimental data, for both D_{self} and D_C. Moreover, as dictated by the imposed transition rates (see Table 1), the nC6 molecules are preferentially located in the channels, separated by intersection sites. This lowers the influence of the nearest neighbours interactions that are found almost negligible even at high occupancy. This slight inflection of the adsorption isotherm reveals a rearrangement of the molecules, due to an entropy loss (Zhu et al. 2001; Millot et al. 1998). This characteristic cannot be reproduced by KMC simulations with fixed transition rates. Furthermore, as shown in Fig. 3, implementing fixed anisotropic transition rates does provide a uniform distribution of the molecules on the three types of sites at low loading (Vlugt et al. 1999; Pascual et al. 2003). Nevertheless, Fig. 3 indicates that while loading increases, molecules spend more time in zigzag channels, which denotes a general movement of the molecules from straight to zigzag channels. This is consistent with the "freezing" of the molecules in zigzag channels, all the more than self-diffusion along zigzag channels is found to be lower than the one in the straight direction (see Fig. 4).

4 KMC simulations of nC6/22DMB binary mixture diffusion

In this section we describe a study of the loading dependence of the binary diffusion of nC6/22DMB mixtures by KMC simulations. In their work on the CH_4/CF_4 system, Paschek and Krishna (2001a) emphasized that KMC simulations underestimated correlation effects. Indeed, their model did not account for the different saturation capacities of the two species, neglecting particle-size effects. They implemented a 24-sites unit cell for both components whereas Skoulidas et al. (2003) results of MD simulations exhibited a saturation capacity of 16 molecules/u.c. for CF_4. Indeed, it would have been technically more complicated to combine a 24-sites unit cell network used for CH_4 with a 16-sites unit cell network as employed afterwards by Krishna et al. (2004b) for the study CF_4 in MFI as a single component. This would have implied to define specific adsorption sites for each component in the network. Furthermore, Paschek and Krishna (2001a) reported that the different species mobilities influence each other although guest-guest interactions were neglected. They noticed strong correlation effects described as particles acceleration/slowing effect. Indeed, the supposed "slow" molecule mobility can be increased while the diffusion of the assumed "fast" molecule is decreased. One can find more details in the above mentioned paper.

In the present work, we propose a model that accounts for the different saturation capacities of both component and for molecular interactions between molecules of both species. In this approach, the 22DMB molecules are only located at the intersection sites with a saturation capacity of 4 molecules/u.c. reported by CBMC simulations (Krishna et al. 2002). Consequently, the representation of the zeolite framework based on the same unit cell as previously (see Fig. 1) is adapted to study the binary diffusion of the nC6/22DMB mixture. nC6 molecules propagate by jumping to either type of site whereas 22DMB molecules only hop from an intersection site to another intersection site provided that the channel site in between is vacant. Therefore, only transition rates along both straight and zigzag channels are necessary for 22DMB. As 22DMB transition rates are not available in the literature, they are defined by (7)

$$\begin{aligned} k_{22DMB,str} &= k_{nC6,str\rightarrow \mathrm{int}}/Q \\ k_{22DMB,zz} &= k_{22DMB,str}/3 \end{aligned} \tag{7}$$

where Q is a parameter that allows to tune 22DMB displacement with respect to nC6 mobility. The ratio of three between transition rates in straight and zigzag channels is suggested by MD simulations of Bouyermaouen and Bellemans (1998) on this kind of alkanes. The transition rates implemented for the nC6 molecules are those estimated for the single component diffusion in the second approach described in the previous section. Moreover, nearest neighbours molecular interactions are taken into account by implementing a refinement of the strategy used for single component investigation. As guest-guest interactions differ according to the considered species, f_{ij} parameters are introduced to simulate all possible types of molecular interactions. Self- and corrected diffusivities were computed for each component by using equations similar to (3) and (4) applied to the case of binary mixture studies. In order to have a better understanding of the cooperation and competition effects occurring in binary mixture diffusion , the impact on diffusivities of parameters such as guest-guest interactions, mixture compositions and concentrations of both linear and double-branched molecules is investigated.

The base case simulation is performed by using $Q = 10^3$, which is motivated by macroscopic values of D_{self} in the range of 10^{-16} and 10^{-13} measured for 22DMB (Jolimaître et al. 2002) and for nC6 (Eic and Ruthven 1989), respectively. No interaction between molecules of the same species is considered. Indeed, the 22DMB molecules are well packed in the intersection sites, separated from each other by a channel, while repulsive interactions between nC6 molecules have a low impact on diffusivities (see single component section). Repulsive interactions between nC6 and 22DMB molecules are implemented as these two alkanes molecules are likely to interact according to their kinetic radius and their location in the lattice.

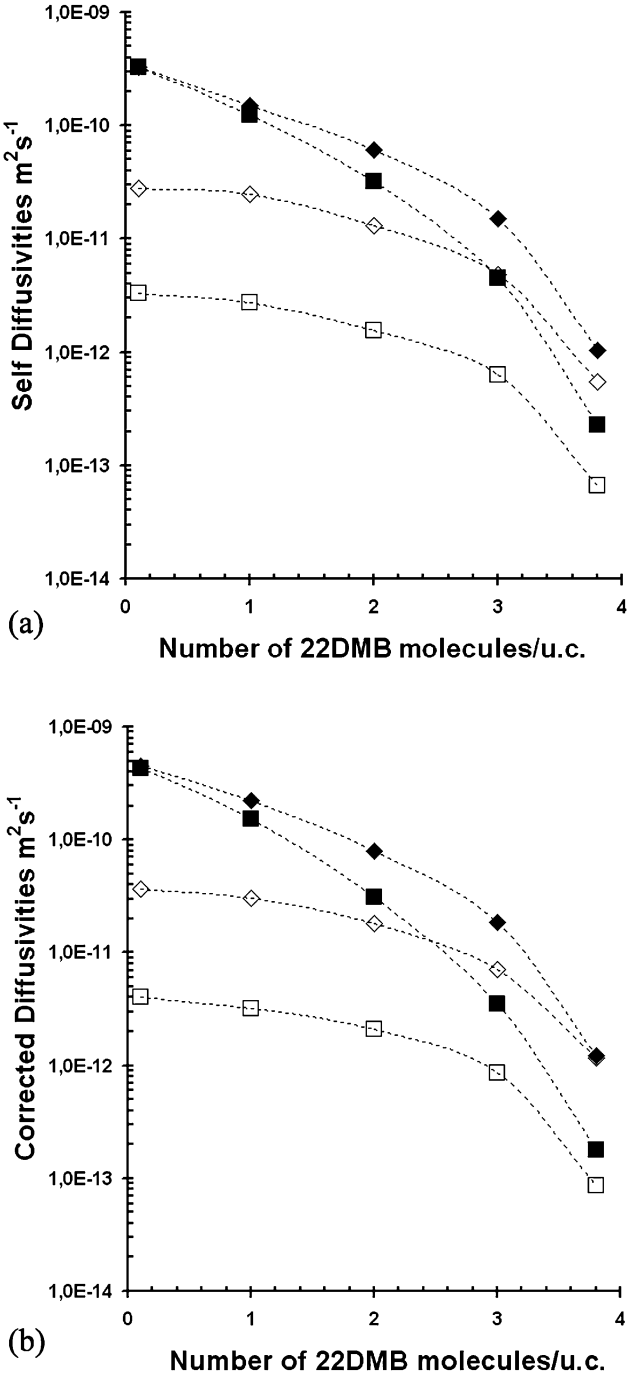

Fig. 5 Self- (**a**) and corrected (**b**) diffusivities of nC6 and 22DMB as a function of number of 22DMB molecules for various Q values. *Filled* and *open symbols* represent diffusivities of nC6 and 22DMB, respectively. *Squares* and *diamonds* correspond to KMC simulations using $Q = 10^3$ and $Q = 10^2$, respectively. In those KMC simulations $\Theta_{nC6} = 2$ is maintained constant and f_{ij} parameters are defined as follows: $f_{nC6/nC6} = 1.0$, $f_{nC6/22DMB} = 3.0$ and $f_{22DMB/22DMB} = 1.0$

A first set of KMC simulations were performed on systems consisting of a fixed concentration of 2 molecules/u.c. of nC6 and a composition of 22DMB varying from 0.1 to 3.8 molecules/u.c. The influence of the Q parameter is in-

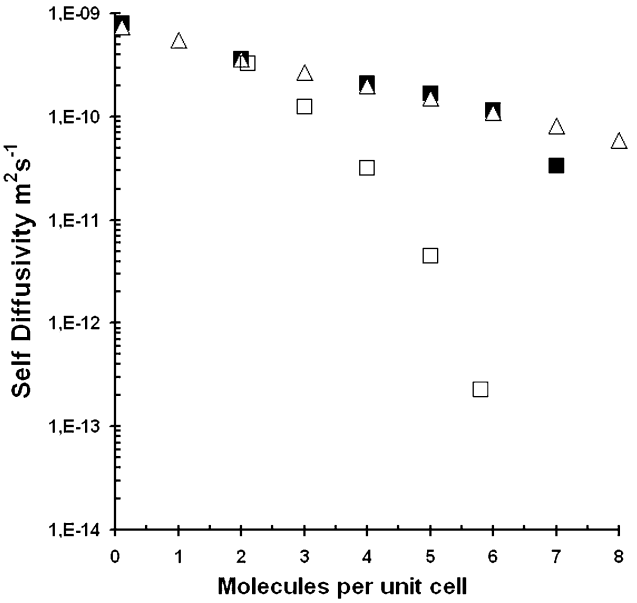

Fig. 6 Different self-diffusivities in $m^2\ s^{-1}$ of nC6 in MFI as a function of the total number of molecules in unit cell. *Filled squares* are experimental QENS measurements of Jobic et al. (2006). *Open triangles* represents the loading dependence of the nC6 self-diffusion as single component represented by the second approach defined in this work. *Open squares* correspond to KMC simulations of binary mixtures containing 2 molecules/u.c. of nC6 and additional 22DMB molecules. In the latter simulations, $Q = 10^3$ and f_{ij} are as follows: $f_{nC6/nC6} = 1.0$, $f_{nC6/22DMB} = 1.0$ and $f_{22DMB/22DMB} = 1.0$

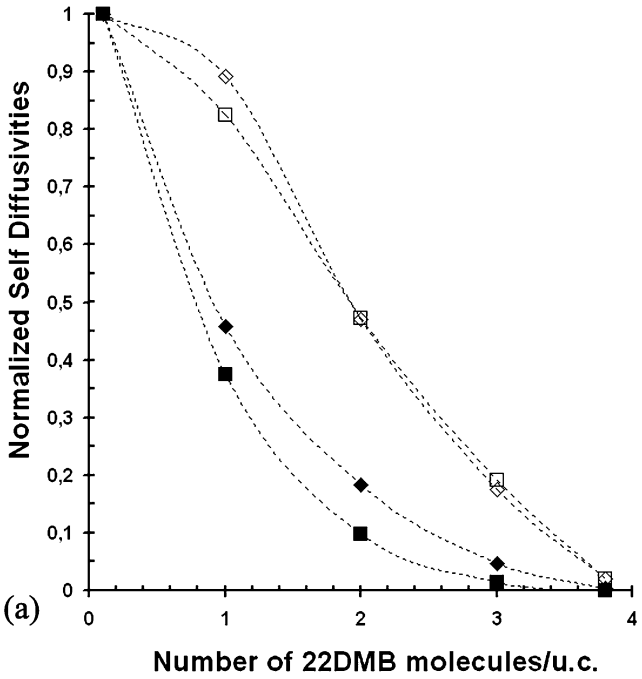

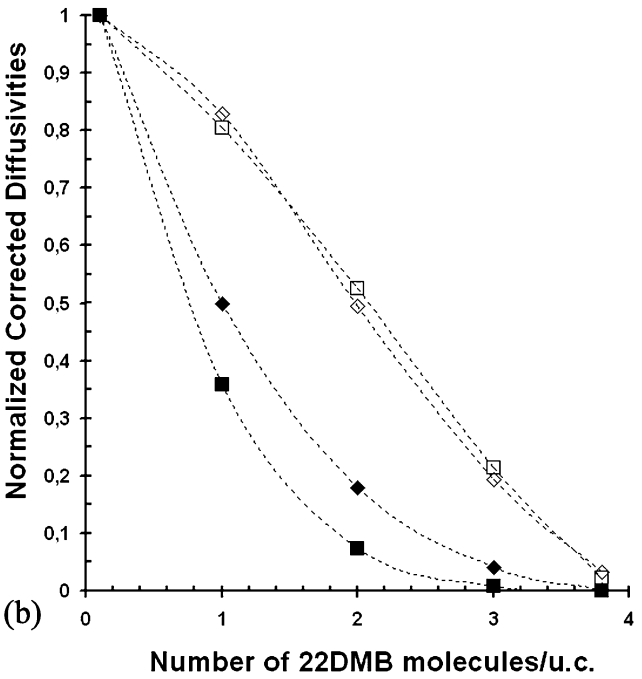

Fig. 7 Normalized self- (**a**) and corrected (**b**) diffusivities of nC6 and 22DMB as a function of 22DMB molecule number. These curves are another representation of the results of Fig. 5 and captions are the same as the one in Fig. 5. The normalizations are realized with respect to results obtained for $\Theta_{22DMB} = 0.1$

vestigated to highlight the impact of the 22DMB transition rates on the nC6 behavior. As shown in Fig. 5, decreasing the parameter Q by one order of magnitude has a significant effect on both D_{self} and D_C of the two components. As expected, decreasing the 22DMB transition rates by one order of magnitude also reduces both D_{self} and D_C of 22DMB by one order of magnitude. It is noticeable that all curves exhibit a sharp reduction for a $\Theta_{22DMB} > 3$. Moreover, whatever the value of Q implemented, the difference between nC6 and 22DMB diffusivities decreases while Θ_{22DMB} increases for both D_{self} and D_C. Near $\Theta_{22DMB,sat}$, the diffusivities of both components are very close to each other, especially concerning corrected diffusivities. Indeed, the number of occupied intersection sites increases while Θ_{22DMB} rises. Since the nC6 molecules have to go trough an intersection site to move on the lattice, their mobility is strongly impaired by the presence of an increasing number of 22DMB molecules "blocking" the intersection sites. Figure 6 shows the self-diffusivities of nC6 as a function of Θ_{nC6}, in the case of nC6 as a single component and in the case of nC6 in presence of 22DMB molecules. The two curves exhibit differences up to three orders of magnitude. Near $\Theta_{22DMB,sat}$, the nC6 molecules have to "wait" for a 22DMB jump to free an intersection site, which explains nC6 diffusivity values close to 22DMB ones at these loadings. The strong impact of 22DMB molecules on nC6 mobility is also highlighted by the large deviation of the normalized self- and corrected diffusivities of nC6 from classical linear decrease (cf. Fig. 7). Moreover, as simulations are performed at a relatively low Θ_{nC6}, the impact of the nC6 molecules on 22DMB mobility is limited. Indeed, both diffusivities of 22DMB presented

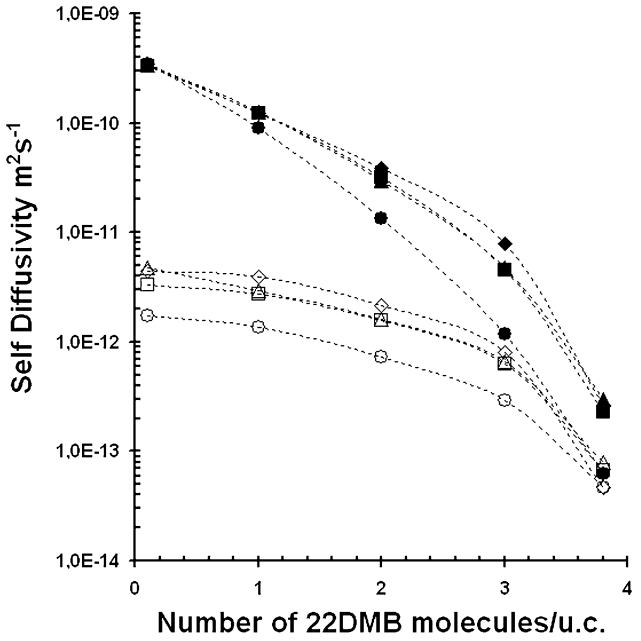

Fig. 8 Self-diffusivities of nC6 and 22DMB as a function of 22DMB molecule number for different values of f_{ij} parameters. *Filled* and *open symbols* represent diffusivities of nC6 and 22DMB, respectively. *Circles* correspond to simulations with $f_{nC6/nC6} = 1.0$, $f_{nC6/22DMB} = 1.0$ and $f_{22DMB/22DMB} = 1.0$. *Squares* correspond to simulations with $f_{nC6/nC6} = 1.0$, $f_{nC6/22DMB} = 3.0$ and $f_{22DMB/22DMB} = 3.0$ (base case). *Triangles* correspond to simulations with $f_{nC6/nC6} = 1.5$, $f_{nC6/22DMB} = 3.0$ and $f_{22DMB/22DMB} = 1.0$. *Diamonds* correspond to simulations with $f_{nC6/nC6} = 1.0$, $f_{nC6/22DMB} = 5.0$ and $f_{22DMB/22DMB} = 1.0$

in Fig. 7 show a classical linear decrease until $\Theta_{22DMB,sat}$. This is characteristic of a strong confinement scenario and typical for KMC simulations that do not account for guest-guest interactions (Paschek and Krishna 2000).

In order to study the influence of molecular interactions, KMC simulations were performed on the system described in the previous paragraph with a fixed value of $Q = 10^3$ by implementing various repulsive interactions via the f_{ij} parameters. The results on the self-diffusivities are shown in Fig. 8. Those on corrected diffusivities are not reported here but follow the same behavior. D_{self} curves display the same general trends as the one exhibited in Fig. 5. The impact of molecular interaction between nC6 molecules ($f_{nC6/nC6}$) is almost negligible, which can be explained by the relatively low nC6 loading as well as the preferential location of the nC6 molecules in the channels, separated by intersection sites (cf. discussion about nC6 as single component). On the contrary, a modification of repulsive interactions between nC6 and 22DMB molecules ($f_{nC6/22DMB}$) generate a variation of D_{self} of both components. This impact is all the more significant on the nC6 self-diffusivities that Θ_{22DMB} and thus the number of possible interactions between the two species raises. Those interactions lead to an increase of the transition rates and thus a rise of the self-diffusivity

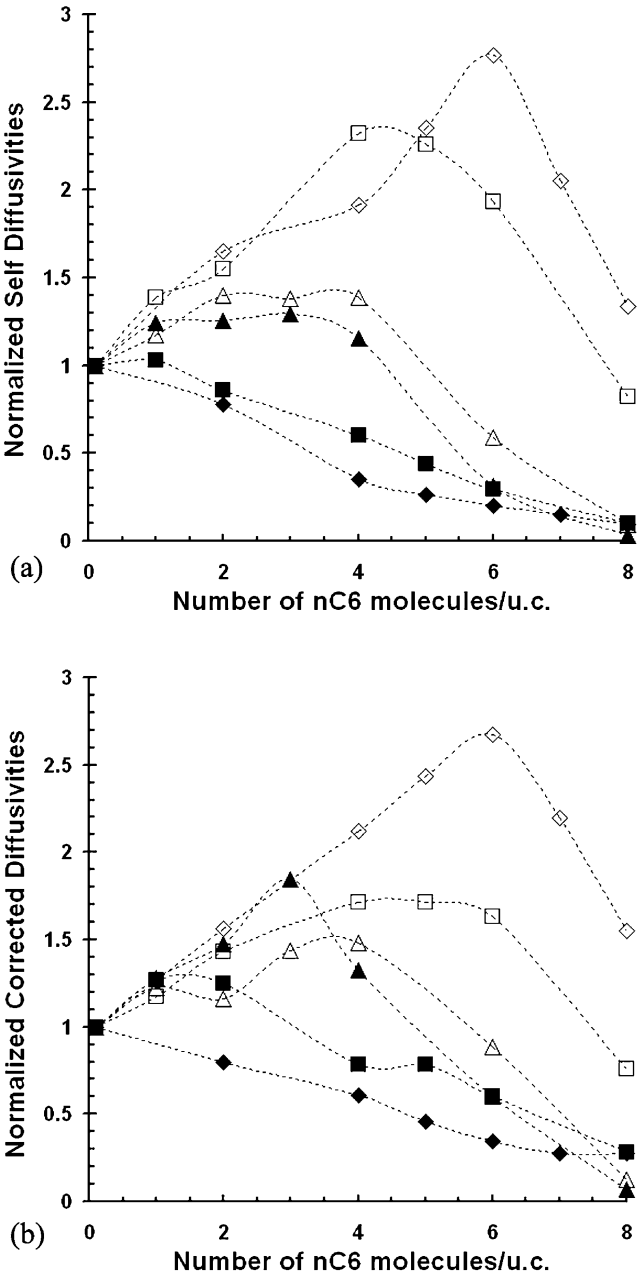

Fig. 9 Normalized self- (**a**) and corrected (**b**) diffusivities of nC6 and 22DMB as a function of number of nC6 molecules for various fixed values of Θ_{22DMB}. *Filled* and *open symbols* represent diffusivities of nC6 and 22DMB, respectively. *Diamonds*, *squares* and *triangles* correspond to KMC simulations realized using $\Theta_{22DMB} = 1.0, 2.0$ and 3.0 respectively using $f_{nC6/nC6} = 1.0$, $f_{nC6/22DMB} = 3.0$ and $f_{22DMB/22DMB} = 1.0$

as already explained. The same effect is not noticed for the self-diffusivity of the double-branched molecule. Above $\Theta_{22DMB} = 3$, the observed sharp reduction of D_{self} of both components observed can be explained by the low amount of vacant intersections.

A second set of KMC simulations were performed by maintaining a constant Θ_{22DMB} and varying the concentra-

tion of nC6 up to saturation. The Q ratio defined by (7) is set to 10^3. Repulsive interactions were only implemented between nC6 and 22DMB. The results for different Θ_{22DMB} are summarized in Fig. 9. The behaviours of both components differ. It is noticeable that both self- and corrected diffusivities of 22DMB increase with Θ_{nC6} until a maximum before sharply diminishing. This maximum is observed for all Θ_{22DMB} values simulated. Besides, it is all the more pronounced that the Θ_{22DMB} is low because of larger number of vacant intersection sites. Indeed, the site blocking effect increases with Θ_{22DMB}, until becoming predominant compared to guest-guest interactions. This confirms the general acceleration of the slow molecules in the presence of fast molecules that as already discussed by Paschek and Krishna (2001a). Different shapes are observed for the self- and corrected nC6 diffusivities. It appears that Θ_{22DMB} has a strong impact on nC6 corrected diffusivity. The impact of correlation effects generated by the presence of 22DMB molecules on the nC6 self-diffusivity arises above $\Theta_{22DMB} = 2$.

5 Conclusion

The loading dependence of single-component diffusion of linear hexane (nC6) in silicalite at 300 K, has been investigated using a KMC model based on original anisotropic transition rates. In order to account for the molecule distribution within the zeolite framework, two different approaches have been developed to this model enclosing adsorption features via the introduction of the Langmuir constants of the DSL model. Moreover, guest-guest interactions are accounted for by using Reed–Ehrlich methodology via the parameter f. The results of these KMC simulations for one of the approaches developed are in good agreement with recent experimental QENS measurements (Jobic et al. 2006), for both D_{self} and D_C. The most suitable approach assumes that the two types of adsorption sites defined by the DSL model are the straight and the zigzag channel sites and considers the intersections sites as "passing" sites. This approach also defines an unfavoured probability of leaving zigzag channel sites while keeping a greater mobility of the molecules in the straight channels. Moreover, a general movement of the molecules from straight to zigzag channels is observed, in accordance with the already-reported incommensurate "freezing" of nC6 in the zigzag channels at intermediate loadings.

The implementation of fixed transition rates drives the nC6 molecules towards channel sites, which lowers the influence of the nearest neighbours interactions. The rearrangement of the molecule positions around 4 molecules/u.c. cannot be reproduced.

The KMC model used for the study of binary diffusion at 300 K of nC6 and 22DMB mixture in silicalite is based on information coming from the single component investigation and accounts for the different saturation capacities of both species. It also allows for all type of molecular interactions to be considered by introducing f_{ij} parameters. As this model only account for nearest neighbours influence, the interactions between molecules of 22DMB are neglected. Results have shown a larger impact of interaction between linear and double-branched molecules than interactions between two linear molecules. Besides, the presence of 22DMB molecules in intersection sites has a significant impact on nC6 self- and corrected diffusivities compared to its behaviour as a single component. Near $\Theta_{22DMB,sat}$, the nC6 diffusivities sharply decreases towards 22DMB diffusivity values due to the reduction of vacant intersection sites.

Acknowledgements The authors are grateful to Prof. S.M. Auerbach for providing scientific support on mean average data calculations. IFP, IRCELYON and ANRT are gratefully acknowledged for their financial support of this work.

References

Auerbach, S.M., Henson, N.J., Cheetham, A.K., Metiu, H.I.: Transport theory for cationic zeolites: diffusion of benzene in Na-Y. J. Phys. Chem. **99**, 10600–10608 (1995)

Bouyermaouen, A., Bellemans, A.: Molecular simulations of the diffusion of n-butane and i-butane in silicalite. J. Chem. Phys. **108**, 2170–2172 (1998)

Cavalcante, C.L.J., Ruthven, D.M.: Adsorption of branched and cyclic paraffins in silicalite. 2. Kinetics. Ind. Eng. Chem. Res. **34**, 185–191 (1995)

Dubbeldam, D., Beerdsen, E., Vlugt, T.J.H., Smit, B.: Molecular simulations of loading-dependent diffusion in nanoporous materials using extended dynamically corrected transition state theory. J. Chem. Phys. **122**, 224712 (2005)

Eic, M., Ruthven, D.M.: Intracrystalline diffusion of linear paraffins and benzene in silicalite studied by the ZLC methods. Stud. Surf. Sci. Catal. **49B**, 897–905 (1989)

Fichthorn, K.A., Weinberg, W.H.: Theoretical foundations of dynamical Monte Carlo simulations. J. Chem. Phys. **95**, 1090–1096 (1991)

Fichthorn, K.A., Weinberg, W.H.: Influence of time-dependent rates of mass transfer on the kinetics of domain growth. Phys. Rev. Lett. **68**, 604–607 (1992)

Frenkel, D., Smit, B.: Understanding Molecular Simulations: From Algorithms to Applications, 2nd edn. Academic, San Diego (2002)

Gergidis, L.N., Theodorou, D.N., Jobic, H.: Dynamics of *n*-butane-methane mixtures in silicalite, using quasi elastic neutron scattering and molecular dynamics simulations. J. Phys. Chem. B **104**, 5541–5552 (2000)

Jobic, H., Laloué, N., Laroche, C., van Baten, J.M., Krishna, R.: Influence of isotherm inflection on the loading dependence of the diffusivities of *n*-hexane and *n*-heptane in MFI zeolite. Quasi elastic neutron scattering experiments supplemented by molecular simulations. J. Phys. Chem. B **110**, 2195–2201 (2006)

Jolimaître, E., Ragil, K., Tayakout-Fayolle, M., Jallut, C.: Separation of mono- and dibranched hydrocarbons on sicalite. AIChe J. **48**, 1927–1937 (2002)

June, R.L., Bell, A.T., Theodorou, D.N.: Transition-state studies of xenon and SF6 diffusion in silicalite. J. Phys. Chem. **95**, 8866–8878 (1991)

June, R.L., Bell, A.T., Theodorou, D.N.: Molecular dynamics studies of butane and hexane in silicalite. J. Phys. Chem. **96**, 1051–1060 (1992)

Keil, F.J., Krishna, R., Coppens, M.O.: Modeling of diffusion in zeolites. Rev. Chem. Eng. **16**(2), 71–197 (2000)

Koriabkina, A.O., de Jong, A.M., Hensen, E.J.M., van Santen, R.A.: Concentration and temperature dependence of the diffusivity of *n*-hexane in MFI-zeolites. Microporous Mesoporous Mater. **77**, 119–129 (2005)

Krishna, R., Calero, S., Smit, B.: Investigation of entropy effects during sorption of mixtures of alkanes in MFI zeolite. Chem. Eng. J. **88**, 81–94 (2002)

Krishna, R., Paschek, D., Baur, R.: Modeling the occupancy dependence of diffusivities in zeolites. Microporous Mesoporous Mater. **76**, 233–246 (2004a)

Krishna, R., van Baten, J.M., Dubbeldam, D.: On the inflection in the concentration dependence of the Maxwell–Stefan diffusivity of CF4 in MFI zeolite. J. Phys. Chem. B **108**, 14820–14822 (2004b)

Leroy, F., Rousseau, B., Fuchs, A.H.: Self-diffusion of *n*-alkanes in silicalite using molecular dynamics simulations: a comparison between rigid and flexible frameworks. Phys. Chem. Chem. Phys. **6**, 775–783 (2004)

Maceiras, D.B., Sholl, D.S.: Analysis of binary transport diffusivities and self-diffusivities in a lattice model for silicalite. Langmuir **18**, 7393–7400 (2002)

Metiu, A.I., Lu, Y.T., Zangh, Z.Y.: Epitaxial growth and the art of computer simulations. Science **255**, 1088–1092 (1992)

Millot, B., Methivier, A., Jobic, H.: Adsorption of *n*-alkanes on silicalite crystals. A temperature-programmed desorption study. J. Phys. Chem. B **102**, 3210–3215 (1998)

Paschek, D., Krishna, R.: Monte Carlo simulations of self- and transport-diffusivities of 2-methylhexane in silicalite. Phys. Chem. Chem. Phys. **2**, 2389–2394 (2000)

Paschek, D., Krishna, R.: Diffusion of binary mixtures in zeolites: kinetic Monte Carlo versus molecular dynamics simulations. Langmuir **17**, 247–254 (2001a)

Paschek, D., Krishna, R.: Kinetic Monte Carlo diffusion of transport diffusivities of binary mixtures in zeolites. Phys. Chem. Chem. Phys. **3**, 3185–3191 (2001b)

Pascual, P., Ungerer, P., Tavitian, B., Pernot, P., Boutin, A., Development of a transferable guest-host force field for adsorption of hydrocarbons in zeolites. I. Reinvestigation of alkane adsorption in silicalite by grand canonical Monte Carlo simulation. Phys. Chem. Chem. Phys. **5**, 3684–3693 (2003)

Reed, A.D., Ehrlich, G.: Surface diffusion, atomic jump rates and thermodynamics. Surf. Sci. **102**, 588–601 (1981)

Runnebaum, R.C., Maginn, E.J.: Molecular dynamics simulations of alkanes in the zeolite silicalite: evidence for resonant diffusion effects. J. Phys. Chem. B **101**, 6394–6408 (1997)

Saravanan, C., Auerbach, S.M: Modeling the concentration dependence of diffusion in zeolites. II. Kinetic Monte Carlo simulations of benzene in Na-Y. J. Chem. Phys. **107**, 8132–8137 (1997)

Shuring, D., Jansen, A.P.J., van Santen, R.A.: Concentration and chain-lenght dependence of the diffusivity of alkanes in zeolites studied with MD simulations. J. Phys. Chem. B **104**, 941–948 (2000)

Skoulidas, I., Sholl, D.S.: Transport diffusivities of CH4, CF4, He, Ne, Ar, Xe and SF6 in silicalite from atomistic simulations. J. Phys. Chem. B **106**, 5058–5067 (2002)

Skoulidas, A.I., Sholl, S., Krishna, R.: Correlation effects in diffusion of CH_4/CF_4 mixtures in MFI zeolite. A study linking MD simulations with the Maxwell–Stefan formulation. Langmuir **19**, 7977–7988 (2003)

Song, L., Rees, L.V.C.: Adsorption and transport of n-hexane in silicalite-1 by the frequency response technique. J. Chem. Soc. Faraday Trans. **93**, 649–657 (1997)

Smit, B., Maesen, T.L.M.: Commensurate 'freezing' of alkanes in the channels of a zeolite. Nature **374**, 42–44 (1995)

Smit, B., Loyens, L.D.J.C., Verbist, G.L.M.M.: Simulation of adsorption and diffusion of hydrocarbons in zeolites. Faraday Discuss. **106**, 93–104 (1997)

Snurr, R.Q., Kärger, J.: Molecular simulations and NMR measurements of binary diffusion in zeolites. J. Phys. Chem. B **101**, 6469–6473 (1997)

Vlugt, T.J.H., Krishna, R., Smit, B.: Molecular simulations of adsorption isotherms for linear and branched alkanes and their mixtures in silicalite. J. Phys. Chem. B **103**, 1102–1118 (1999)

Zhu, W., Kapteijn, F., van der Linden, B., Moulijn, J.A.: Equilibirum adsorption of linear and branched C6 alkanes on silicalite-1 studied by the tapered element oscillating microbalance. Phys. Chem. Chem. Phys. **3**, 1755–1761 (2001)